

# Rydberg antiblockade with resonant dipole-dipole interactions

Shi-Lei Su

*School of Physics, Zhengzhou University, Zhengzhou 450001, China*

We perform a comprehensive investigation of the resonant Rydberg dipole-dipole interaction based antiblockade regimes for different Rydberg-Rydberg interaction types that have been observed in experiment. By using the dressed state method, the laser coupled terms were rewritten with respect to the dressed state formed by the strong and resonant dipole-dipole interaction, based on which we can calculate the effective dynamics and further get the Rydberg antiblockade (RAB) condition. We then study the possible applications of the proposed RAB regimes, including the geometric quantum computation, dissipative dynamics based entanglement preparation, and possible applications in some physical parameters estimation. Our study enriches the RAB regime since it goes beyond the usual vdW-type based RAB, and may be get more attention for the experimental and theoretical study in neutral atoms in the near future.

## I. INTRODUCTION

Long-range interaction would be exhibited between highly excited Rydberg atoms with principal quantum number  $n \gg 1$  due to their large dipole moment [1]. Due to this unique property, trapped Rydberg atoms have been extensively utilized to accomplish quantum logic gate [2–6] based on Rydberg blockade, i.e., the excitation of ground-state neutral atoms to the Rydberg state would be prohibited if they are in the blockade radius of an highly excited neutral atom. Recent experiments have demonstrated quantum logic gates between single Rydberg atoms based on Rydberg blockade [7–16].

In contrast to Rydberg blockade, the interaction-induced excitation enhancement in an ultracold lattice gas was studied and defined as “Rydberg antiblockade” (RAB) [17]. And Ref. [18] demonstrated the RAB in experiment even the atomic interaction shift is much greater than the excitation line width when the system is initially set as an unstructured gas. Then, under the condition that dipole-dipole Rydberg-Rydberg-interaction (RRI) strength  $V_d$  is much smaller than driving Rabi frequency  $\Omega$  ( $V_d \gg \Omega$ ), Ref. [19] showed that once the dark state which contains three excited Rydberg atoms was populated, it would keep invariant. The two-qubit case of the atoms are interacting with a zero-area phase-jump pulse was also studied in Ref. [20]. Besides, under the parameter range  $V_d \sim \Omega$ , the dynamics that two-excitation Rydberg states involve in the evolution are also discussed to limit the blockade error [21]. Along with development of the technology in optical control [22], microwave control [23–28] and electric field control [3, 29–43] of the resonant dipole-dipole RRI, the implementation of these schemes may also be guaranteed.

In fact, with the condition  $V_v \ll \Omega$ , where  $V_v$  denotes van der Waals (vdW)-type RRI strength, the two-atom-excitation was considered earlier for the construction of quantum logic gate in Ref. [2]. Also, the RAB was studied under the condition  $V_v \gg \Omega$  [44, 45], and has been studied for motional effects [46], dissipative dynamics [47–49], periodically driving [50] as well as construction of quantum gates [51]. Very recently, RAB was

also studied in strongly interacting Rydberg atom experiment [52], trapped Rydberg ion chain [53], and cold atom ensemble [54].

In this manuscript, we would perform comprehensive investigations for the resonant dipole-dipole-RRI-based antiblockade under the regime  $V_d \gg \Omega$  and briefly discuss its applications. The resonant two-body dipole-dipole RRIs modulated by the external fields can be roughly classified as the following types. The first type is the Förster resonance, such as  $|d\rangle|d\rangle \leftrightarrow |p\rangle|f\rangle+|f\rangle|p\rangle$  [24, 33–35], and  $|p\rangle|p\rangle \leftrightarrow |s\rangle|s'\rangle+|s'\rangle|s\rangle$  [36, 38]. The second type is “spin-exchange”-type RRI interaction  $|s\rangle|p\rangle \leftrightarrow |p\rangle|s\rangle$  [37],  $|p\rangle|d\rangle \leftrightarrow |d\rangle|p\rangle$  [55] or  $|s\rangle|p'\rangle \leftrightarrow |p\rangle|s'\rangle$  [28]. And the third type is “collective exchange”-type RRI,  $|s\rangle|s'\rangle \leftrightarrow |p\rangle|p'\rangle$  [36, 39–42] or  $|d\rangle|d'\rangle \leftrightarrow |f\rangle|f'\rangle$  [43]. In addition, there may be another form of RRI type,  $|p\rangle|p'\rangle \leftrightarrow |s\rangle|d\rangle$  [31] or  $|d\rangle|d'\rangle \leftrightarrow |p\rangle|f\rangle$  [43]. The strong dipole-dipole interactions facilitate the dressed states, based on which we show how to achieve the RAB for all of the above mentioned resonant types.

The rest content of the manuscript is organized as follows: In Sec. II, we illustrate the basic theory of the manuscript, including the models extracted from experiment and the dressed state method. In Sec. III, we study how to achieve the RAB regime and plot the population evolution dynamics with the models shown in Sec. II. In Sec. IV, we show the potential applications of the proposed RAB with one model as an example. The conclusion is given in Sec. V.

## II. BASIC THEORY

### A. Models

As shown in Fig. 1, we consider how to achieve the effective RAB dynamical process (a) for three types of resonant dipole-dipole interactions (b) (c) and (d), respectively, with dressed state method. For panel (b), we consider the experimental configuration [34]  $|p\rangle \equiv |61P_{1/2}, m_J = 1/2\rangle$ ,  $|d\rangle \equiv |59D_{3/2}, m_J = 3/2\rangle$  and  $|f\rangle \equiv |57F_{5/2}, m_J = 5/2\rangle$  of two  $^{87}\text{Rb}$  atoms. By ap-

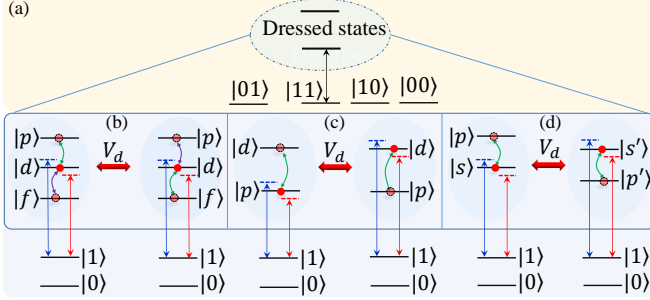


FIG. 1. The diagrammatic sketch of the RAB with resonant dipole-dipole interaction. (a) The effective dynamics under two-atom basis with dressed states. Panels (b) (c) and (d) show the laser drivings to achieve the RAB for the förster resonance, ‘‘spin exchange’’ and ‘‘collective exchange’’ RRIs, respectively.  $V_d$  means the RRI strength.  $|s\rangle, |s'\rangle, |p\rangle, |d\rangle$  and  $|f\rangle$  denote Rydberg states.  $|0\rangle$  and  $|1\rangle$  are two ground states. For simplicity, we label the left atom as atom 1 and the right atom as atom 2 throughout this manuscript for panels (b), (c) and (d).

plying an electric fields  $\epsilon \simeq 32$  mV cm $^{-1}$ , these Rydberg states can be brought to exact resonance with  $C_3 = 2.54$  GHz  $\mu\text{m}^3$ . One of the states in computational space is chosen as  $|1\rangle \equiv |5S_{1/2}, F = 2, m_F = 2\rangle$  [34] and the other states  $|0\rangle$  in computational subspace is decoupled with the excitation process and may be chosen as  $|0\rangle \equiv |5S_{1/2}, F = 1, m_F = 0\rangle$ . The excitation is accomplished by two-photon process with two lasers of wavelengths 795 nm( $\pi$  polarization) and 474 nm( $\sigma_+$  polarization) [34].

For panel (c), we consider the experimental configuration as [55]  $|d\rangle \equiv |62D_{3/2}, m_J = 3/2\rangle$ ,  $|p\rangle \equiv |63P_{1/2}, m_J = 1/2\rangle$ . These two Rydberg states are resonant with each other and  $C_3 = 7.965$  GHz  $\mu\text{m}^3$ . One of the ground states are chosen as  $|1\rangle \equiv |5S_{1/2}, F = 2, m_F = 2\rangle$  [55] and the rest computational state can be chosen as  $|0\rangle \equiv |5S_{1/2}, F = 1, m_F = 0\rangle$ . The excitation process from  $|1\rangle$  to state  $|d\rangle$  is accomplished by two-photon transition with wavelengths 795 nm ( $\pi$  polarization) and 474 nm ( $\sigma_+$  polarization), respectively. In this manuscript, we also consider the single-photon excitation process from  $|1\rangle$  to  $|p\rangle$  [55].

For panel (d), we consider the experimental configuration as [39],  $|s\rangle \equiv |48S_{1/2}, m_J = 1/2\rangle$ ,  $|p\rangle \equiv |48P_{1/2}, m_J = 1/2\rangle$ ,  $|s'\rangle \equiv |50S_{1/2}, m_J = 1/2\rangle$ ,  $|p'\rangle \equiv |49P_{1/2}, m_J = 1/2\rangle$ . These states are resonant with each other when the electric fields  $\epsilon = 710$  mV cm $^{-1}$  and the value of  $C_3$  is about 0.6 GHz  $\mu\text{m}^3$ . Two ground states in computational subspace can be chosen as  $|1\rangle \equiv |5S_{1/2}, F = 2, m_F = 0\rangle$  and  $|0\rangle \equiv |5S_{1/2}, F = 1, m_F = 0\rangle$  [39]. The excitation process from  $|1\rangle$  to  $|s\rangle$  or  $|s'\rangle$  can be implemented by two-photon process [39].

## B. Dressed states

To show the basis of dressed states, we here temporarily consider Hamiltonian

$$\hat{H} = \hat{H}_\Omega + \hat{H}_d, \quad (1)$$

where  $\hat{H}_\Omega = \sum_{k=1}^2 \Omega/2|1\rangle_k \langle R| + \text{H.c.}$  denote the excitation process from  $|1\rangle$  to Rydberg state and  $\hat{H}_d = V_d|Rr\rangle \langle rR|$  denotes the resonant dipole-dipole interactions. If  $V_d \gg \Omega$ , the eigenstates of  $\hat{H}_v$ , i.e.,  $|\Pi_\pm\rangle$  with eigenvalues  $E_\pm$ , can be used to rewrite Eq. (1) as

$$\hat{H} = \sum_{j=+,-} \hat{H}_\Omega |\Pi_j\rangle \langle \Pi_j| + E_j |\Pi_j\rangle \langle \Pi_j|. \quad (2)$$

For concrete Rydberg atom system, one can calculate the first term of Eq. (2) and rotate with respect to the second term to see the systematic dynamics more clearly and further choose parameters to achieve the desired dynamics. In this process,  $|\Pi_\pm\rangle$  can be called as dressed states.

## III. RYDBERG ANTIBLOCKADE WITH RESONANT DIPOLE-DIPOLE INTERACTIONS

### A. RAB with förster resonance

As shown in Fig. 1(b), consider two Rydberg atoms and each atom has two ground states  $|0\rangle$  and  $|1\rangle$ , and three Rydberg states  $|s\rangle, |p\rangle$  and  $|d\rangle$ . Bichromatic classical fields are imposed on these two atoms to off-resonantly drive the transition  $|1\rangle \leftrightarrow |d\rangle$  with an identical Rabi frequency  $\Omega$  but opposite detuning  $\Delta$  through two-photon process. After the rotating-wave approximation, the Hamiltonian for this concrete system can be written as (let  $\hbar = 1$ )

$$\begin{aligned} \hat{H}_\Omega &= \frac{\Omega}{2} (e^{i\Delta t} + e^{-i\Delta t}) (|1\rangle_1 \langle d| + |1\rangle_2 \langle d|) + \text{H.c.} \\ \hat{H}_d &= \sqrt{2}V_d|dd\rangle \langle r_{pf}| + \text{H.c.} \end{aligned} \quad (3)$$

where  $|mn\rangle$  denotes the abbreviation of  $|m\rangle_1 \otimes |n\rangle_2$  and would be used throughout this manuscript.  $|r_{pf}\rangle$  is defined as  $|r_{pf}\rangle \equiv (|pf\rangle + |fp\rangle)/\sqrt{2}$ . Following the process in Sec. II B, one can diagonalize  $\hat{H}_d$  as  $\sqrt{2}V_d(|+\rangle \langle +| - |-\rangle \langle -|)$  with  $|\pm\rangle \equiv (|dd\rangle \pm |r_{pf}\rangle)/\sqrt{2}$ . Then the Hamiltonian can be written as

$$\begin{aligned} \hat{H}_\Omega &= \frac{\Omega}{\sqrt{2}} (e^{i\Delta t} + e^{-i\Delta t}) [|11\rangle \langle \Psi| + \frac{1}{\sqrt{2}} |\Psi\rangle (\langle +| + \langle -|)] \\ &\quad + \frac{\Omega}{2} (e^{i\Delta t} + e^{-i\Delta t}) (|01\rangle \langle 0d| + |10\rangle \langle d0|) + \text{H.c.} \\ \hat{H}_d &= \sqrt{2}V_d(|+\rangle \langle +| - |-\rangle \langle -|), \end{aligned} \quad (4)$$

in which  $|\Psi\rangle \equiv (|1d\rangle + |d1\rangle)/\sqrt{2}$ . When  $\Delta = 0$ , Hamiltonian  $\hat{H}_\Omega$  itself describes resonant interactions. However, when  $V_d \gg \Omega$  is satisfied, after rotating the total Hamiltonian  $\hat{H}$  with respect to  $\hat{H}_d$ , one can see that the two-excitation Rydberg states would be coupled off-resonantly with large detuning. Thus the Rydberg blockade is produced. In the following we would show how to

achieve the RAB even when  $V_d \gg \Omega$ .

More clearly, we here introduce an energy operator  $\hat{h} \equiv \delta(|+\rangle\langle+| - |-\rangle\langle-|)$  to perform the unitary operation  $\hat{U}_0 = \exp(i\hat{h}t)$  so that the total Hamiltonian  $\hat{H}_\Omega + \hat{H}_d$  becomes [50, 56]

$$\hat{\mathcal{H}} = \left\{ \frac{\Omega}{2} \left[ \sqrt{2} (e^{i\Delta t} + e^{-i\Delta t}) |11\rangle\langle\Psi| + \left( e^{i(\Delta-\delta)t} + e^{-i(\Delta+\delta)t} \right) |\Psi\rangle\langle+| + \left( e^{i(\Delta+\delta)t} + e^{-i(\Delta-\delta)t} \right) |\Psi\rangle\langle-| \right. \right. \\ \left. \left. + (e^{i\Delta t} + e^{-i\Delta t}) (|01\rangle\langle 0d| + |10\rangle\langle d0|) \right] + \text{H.c.} \right\} + \hat{H}_d - \hat{h} \quad (5)$$

If  $\{\Delta, \Delta \pm \delta\} \gg \Omega$ ,  $\delta = 2\Delta$  and the RAB condition  $V_d = \sqrt{2}\Delta - \Omega^2/(3\sqrt{2}\Delta)$  are satisfied, the effective Hamiltonian can be finally achieved.

$$\hat{H}_e = \frac{\Omega^2}{2\Delta} |11\rangle\langle r_{pf}| + \text{H.c.} \quad (6)$$

From Eq. (6), one can see that the collective ground state  $|11\rangle$  is resonantly coupled with two-excitation Rydberg state  $|r_{pf}\rangle$  with the effective Rabi frequency  $\Omega_{\text{eff}} \equiv \Omega^2/\Delta$ , which indicates that the RAB is achieved under the case of förster resonance.

Here we should mention that in Ref. [34], the ground state  $|gg\rangle$  (Corresponding to  $|11\rangle$  in our manuscript) is excited to Rydberg state  $|dd\rangle$  firstly via  $\pi$  pulse through the detuned laser. Then the electric field is tuned to make state  $|dd\rangle$  resonant with  $(|pf\rangle + |fp\rangle)/\sqrt{2}$ . In this subsection of our manuscript, we consider the strong förster resonant interactions from beginning to end, and designed schemes to achieve the Rabi oscillation from collective ground state to two-excitation Rydberg state  $(|pf\rangle + |fp\rangle)/\sqrt{2}$ . Meanwhile, the states  $|00\rangle$ ,  $|01\rangle$  and  $|10\rangle$  are decoupled with the two-excitation Rydberg states, which is very convenient to apply this model to the quantum information processing field.

## B. RAB with “spin-exchange” interaction

As shown in Fig. 1(c), consider Rydberg atoms with two ground states  $|0\rangle$  and  $|1\rangle$ , and two Rydberg states  $|p\rangle$  and  $|d\rangle$ . For left(right) Rydberg atom, bichromatic classical fields are imposed to off-resonantly drive the transition  $|1\rangle \leftrightarrow |p(d)\rangle$  through single(two)-photon process with an identical Rabi frequency  $\Omega$  but opposite detuning  $\Delta$ . After the rotating-wave approximation, the Hamiltonian for this concrete system can be written as (let  $\hbar = 1$ )

$$\hat{H}_\Omega = \frac{\Omega}{2} (e^{i\Delta t} + e^{-i\Delta t}) (|1\rangle_1\langle p| + |1\rangle_2\langle d|) + \text{H.c.} \\ \hat{H}_d = V_d |pd\rangle\langle dp| + \text{H.c.} \quad (7)$$

Through using the dressed states  $|\tilde{\pm}\rangle \equiv (|pd\rangle \pm |dp\rangle)/\sqrt{2}$ , one can rewrite Eq. (7) as

$$\hat{H}_\Omega = \frac{\Omega}{\sqrt{2}} (e^{i\Delta t} + e^{-i\Delta t}) [|11\rangle\langle\Phi| + \frac{1}{\sqrt{2}} |\Phi\rangle(\langle\tilde{+}| + \langle\tilde{-}|)] \\ + \frac{\Omega}{2} (e^{i\Delta t} + e^{-i\Delta t}) (|01\rangle\langle 0d| + |10\rangle\langle d0|) + \text{H.c.}$$

$$\hat{H}_d = V_d (|\tilde{+}\rangle\langle\tilde{+}| - |\tilde{-}\rangle\langle\tilde{-}|) \quad (8)$$

with  $|\Phi\rangle \equiv (|1d\rangle + |p1\rangle)/\sqrt{2}$ . Follow the similar process in Sec. III A, if the relation  $\Delta \gg \Omega$  and RAB condition  $V_d = 2\Delta - \Omega^2/(3\Delta)$  are satisfied, one can get the effective Hamiltonian as

$$\hat{H}_e = \frac{\Omega^2}{2\Delta} |11\rangle\langle dp| + \text{H.c.}, \quad (9)$$

which means the Rabi oscillation between collective ground state  $|11\rangle$  and two-excitation Rydberg state  $|pf\rangle$  emerges and the RAB would be implemented if  $\Omega^2 t/\Delta = \pi$  is fulfilled.

Now we discuss the differences of excitation process between our scheme and that in Ref. [55]. In Ref. [55], the atoms are excited step by step. Firstly, one of the Rydberg atoms is excited to  $|d\rangle$  state through two-photon process. Then the state of the excited Rydberg atom is transferred from  $|d\rangle$  to  $|p\rangle$  through microwave field. Immediately, the rest Rydberg atom is excited to state  $|d\rangle$  with  $\Omega \simeq 5.76V_d$  and along with this process the spin-exchange process also happens. The blockade effect in Ref. [55] does not work because  $V_d$  is less than  $\Omega$ . For our scheme in Sec. III B, by using the dressed state method and appropriately choosing parameters, RAB can be accomplished in one step with the condition  $V_d \gg \Omega$ .

## C. RAB with “collective-exchange” interaction

As shown in Fig. 1(d), consider two Rydberg atoms, each has two ground states  $|0\rangle$  and  $|1\rangle$ . The left (right) atom has two Rydberg states  $|s(s')\rangle$  and  $|p(p')\rangle$ . The bichromatic classical fields are imposed to off-resonantly drive the transition  $|1\rangle \leftrightarrow |s(s')\rangle$  through two-photon

process with an identical Rabi frequency  $\Omega$  but opposite detuning  $\Delta$ . With the consideration of rotating-wave approximation and set the electric field strength  $\epsilon = 710$  mV cm $^{-1}$ , the Hamiltonian for this concrete system can be written as (let  $\hbar = 1$ )

$$\begin{aligned}\hat{H}_\Omega &= \frac{\Omega}{2} (e^{i\Delta t} + e^{-i\Delta t}) (|1\rangle_1\langle s| + |1\rangle_2\langle s'|) + \text{H.c.} \\ \hat{H}_d &= V_d|ss'\rangle\langle pp'| + \text{H.c.}\end{aligned}\quad (10)$$

Through using the dressed states  $|\pm\rangle \equiv (|ss'\rangle \pm |pp'\rangle)/\sqrt{2}$ , one can rewrite Eq. (10) as

$$\begin{aligned}\hat{H}_\Omega &= \frac{\Omega}{\sqrt{2}} (e^{i\Delta t} + e^{-i\Delta t}) [|11\rangle\langle \Xi| + \frac{1}{\sqrt{2}}|\Xi\rangle(\langle +' | + \langle -' |)] \\ &\quad + \frac{\Omega}{2} (e^{i\Delta t} + e^{-i\Delta t}) (|01\rangle\langle 0s'| + |10\rangle\langle s0|) + \text{H.c.} \\ \hat{H}_d &= V_d(|+' \rangle\langle +'| - |-' \rangle\langle -'|)\end{aligned}\quad (11)$$

with  $|\Xi\rangle \equiv (|1s'\rangle + |s1\rangle)/\sqrt{2}$ . Follow the similar process in Sec. III A, if the parameters satisfy the relations  $\Delta \gg \Omega$  and RAB condition  $V_d = 2\Delta - \Omega^2/(3\Delta)$ , one can get the effective Hamiltonian as

$$\hat{H}_e = \frac{\Omega^2}{2\Delta} |11\rangle\langle pp'| + \text{H.c.}, \quad (12)$$

which means the Rabi oscillation between collective ground state  $|11\rangle$  and two-excitation Rydberg state  $|pp'\rangle$  emerges and the RAB would be implemented if  $\Omega^2 t/\Delta = \pi$  is fulfilled. In addition to the cases discussed above, the RAB with the resonant dipole-dipole interaction type in Ref. [31, 43] can also be constructed in the similar way.

In Ref. [39], optically trapped cloud of  $2 \times 10^4$   $^{87}\text{Rb}$  gate and source atoms are used for studying the enhancement of single-photon nonlinearity. At zero electric field, the interaction between the  $|ss'\rangle$  pair which is of vdW type and much less than the dipole-dipole interaction  $|ss'\rangle\langle pp'|$ . Thus the collective ground state can be excited to  $|ss'\rangle$  and the single-photon nonlinearity was observed to be enhanced by electrically tuning  $|ss'\rangle$  and  $|pp'\rangle$  pair states into resonant interactions [39]. In this subsection, the resonant dipole-dipole interaction is an initial consideration and on that basis we design the pulse to achieve the RAB in one step with the condition  $V_d \ll \Omega$ .

#### D. Dynamics with partial experimental parameters

In this subsection, we discuss the dynamics of the proposed RAB schemes through numerically solving the master equation

$$\dot{\hat{\rho}} = i[\hat{\rho}, \hat{H}] + \frac{1}{2} \sum_k [2\hat{\mathcal{L}}_k \hat{\rho} \hat{\mathcal{L}}_k^\dagger - \hat{\mathcal{L}}_k^\dagger \hat{\mathcal{L}}_k \hat{\rho} - \hat{\rho} \hat{\mathcal{L}}_k^\dagger \hat{\mathcal{L}}_k] \quad (13)$$

where  $\rho$  denote the density matrix of system state,  $\hat{\mathcal{L}}_k$  is the  $k$ -th Lindblad operator described the dissipation process, and  $\hat{H}$  is the initial Hamiltonian of the whole

system. For the model in Sec. III A, the full Hamiltonian is  $\hat{H} = \hat{H}_\Omega + \hat{V}_d$  that have been shown in Eq. (3). The lifetimes for  $|p\rangle$ ,  $|d\rangle$  and  $|f\rangle$  are about 0.53 ms, 0.22 ms and 0.13 ms respectively [57, 58]. The Lindblad operators are  $\hat{\mathcal{L}}_1 = \sqrt{\gamma_p/2}|0\rangle_1\langle p|$ ,  $\hat{\mathcal{L}}_2 = \sqrt{\gamma_p/2}|1\rangle_1\langle p|$ ,  $\hat{\mathcal{L}}_3 = \sqrt{\gamma_d/2}|0\rangle_1\langle d|$ ,  $\hat{\mathcal{L}}_4 = \sqrt{\gamma_d/2}|1\rangle_1\langle d|$ ,  $\hat{\mathcal{L}}_5 = \sqrt{\gamma_f/2}|0\rangle_1\langle f|$ ,  $\hat{\mathcal{L}}_6 = \sqrt{\gamma_f/2}|1\rangle_1\langle f|$ ,  $\hat{\mathcal{L}}_7 = \sqrt{\gamma_p/2}|0\rangle_2\langle p|$ ,  $\hat{\mathcal{L}}_8 = \sqrt{\gamma_p/2}|1\rangle_2\langle p|$ ,  $\hat{\mathcal{L}}_9 = \sqrt{\gamma_d/2}|0\rangle_2\langle d|$ ,  $\hat{\mathcal{L}}_{10} = \sqrt{\gamma_d/2}|1\rangle_2\langle d|$ ,  $\hat{\mathcal{L}}_{11} = \sqrt{\gamma_f/2}|0\rangle_2\langle f|$ ,  $\hat{\mathcal{L}}_{12} = \sqrt{\gamma_f/2}|1\rangle_2\langle f|$ , where  $\gamma_j$  denotes the atomic spontaneous emission rate. For the model in Sec. III B, the full Hamiltonian is shown in Eq. (7). The lifetimes for  $|p\rangle$  and  $|d\rangle$  are about 0.59 ms and 0.25 ms respectively [57, 58]. The Lindblad operators are  $\hat{\mathcal{L}}_1 = \sqrt{\gamma_p/2}|0\rangle_1\langle p|$ ,  $\hat{\mathcal{L}}_2 = \sqrt{\gamma_p/2}|1\rangle_1\langle p|$ ,  $\hat{\mathcal{L}}_3 = \sqrt{\gamma_d/2}|0\rangle_1\langle d|$ ,  $\hat{\mathcal{L}}_4 = \sqrt{\gamma_d/2}|1\rangle_1\langle d|$ ,  $\hat{\mathcal{L}}_5 = \sqrt{\gamma_p/2}|0\rangle_2\langle p|$ ,  $\hat{\mathcal{L}}_6 = \sqrt{\gamma_p/2}|1\rangle_2\langle p|$ ,  $\hat{\mathcal{L}}_7 = \sqrt{\gamma_d/2}|0\rangle_2\langle d|$ ,  $\hat{\mathcal{L}}_8 = \sqrt{\gamma_d/2}|1\rangle_2\langle d|$ . For the model in Sec. III C, the full Hamiltonian is shown in Eq. (10). The lifetimes for  $|s\rangle$ ,  $|s'\rangle$ ,  $|p\rangle$  and  $|p'\rangle$  are about 0.12 ms, 0.13 ms, 0.25 ms and 0.27 ms, respectively [57, 58]. The Lindblad operators are  $\hat{\mathcal{L}}_1 = \sqrt{\gamma_s/2}|0\rangle_1\langle s|$ ,  $\hat{\mathcal{L}}_2 = \sqrt{\gamma_s/2}|1\rangle_1\langle s|$ ,  $\hat{\mathcal{L}}_3 = \sqrt{\gamma_p/2}|0\rangle_1\langle p|$ ,  $\hat{\mathcal{L}}_4 = \sqrt{\gamma_p/2}|1\rangle_1\langle p|$ ,  $\hat{\mathcal{L}}_5 = \sqrt{\gamma_{s'}/2}|0\rangle_2\langle s'|$ ,  $\hat{\mathcal{L}}_6 = \sqrt{\gamma_{s'}/2}|1\rangle_2\langle s'|$ ,  $\hat{\mathcal{L}}_7 = \sqrt{\gamma_{p'}/2}|0\rangle_2\langle p'|$ ,  $\hat{\mathcal{L}}_8 = \sqrt{\gamma_{p'}/2}|1\rangle_2\langle p'|$ .

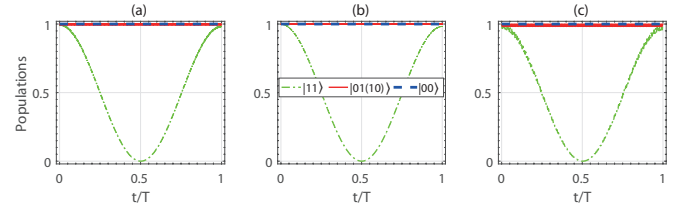


FIG. 2. (a)[(b), (c)] Population of the states for RAB scheme in Sec. III A, (III B, III C) under one evolution period  $T$  with the consideration of atomic spontaneous emission. Parameters are chosen as  $\Omega = 2\pi \times 5$  MHz and  $\Delta$  is set to satisfy the antiblockade condition. For (a)[(b),(c)], the inter-atomic distance is set as 3  $\mu\text{m}$ (3  $\mu\text{m}$ , 2  $\mu\text{m}$ ).

#### IV. POTENTIAL APPLICATIONS OF THE PROPOSED RAB

In this section, for simplicity we only consider the RAB in Sec. III A, based on which one can generalize the applications to other RRI cases.

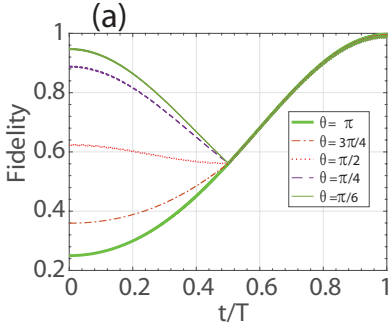


FIG. 3. (a) Evolution of the fidelity of the geometric controlled-arbitrary-phase gate with the consideration of dissipation and the parameters are the same as that in Fig. 2(a). (b) Bloch sphere representation for the conceptual explanation of geometric quantum operation.

### A. Geometric gate with unitary dynamics

We now consider how to construct the controlled-arbitrary-phase geometric gate with the form as

$$\hat{U}_{\text{CP}} = \begin{pmatrix} 1 & 0 & 0 & 0 \\ 0 & 1 & 0 & 0 \\ 0 & 0 & 1 & 0 \\ 0 & 0 & 0 & e^{i\theta} \end{pmatrix}. \quad (14)$$

in the computational space  $\{|00\rangle, |01\rangle, |10\rangle, |11\rangle\}$ . By modulating the Rabi frequencies of the initial Hamiltonian at the half evolution time  $T/2$  appropriately, one can change the effective Hamiltonian in the time interval  $[T/2, T]$  as

$$\hat{H}_e = \frac{e^{i\theta}\Omega^2}{2\Delta} |11\rangle\langle r_{pf}| + \text{H.c.}, \quad (15)$$

Based on which the desired gate can be achieved.

The fidelity of the gate with specific  $\theta$  is shown in Fig. 3(a) by numerically solving the master equation with initial Hamiltonian, in which the initial state is set as  $|\psi(0)\rangle = (|00\rangle + |01\rangle + |10\rangle + |11\rangle)/4$  and the ideally final state is get as  $|\psi(t)\rangle = \hat{U}|\psi(0)\rangle$ . With the consideration of dissipation, the final fidelity are 0.9969, 0.9962, 0.9949, 0.9938 and 0.9936 when  $\theta$  equals  $\pi, 3\pi/4, \pi/2, \pi/4$  and  $\pi/6$ , respectively. The geometric feature of the phase can be easily verified since  $|11\rangle \rightarrow |r_{pf}\rangle \rightarrow e^{i\theta}|11\rangle$  is achieved and  $\langle \Psi_j | \hat{H}_e | \Psi_k \rangle = 0$  [59–63] is satisfied, where  $|\Psi_j\rangle$  ( $|\Psi_k\rangle$ ) is any one of the four states in  $\{|00\rangle, |01\rangle, |10\rangle, |11\rangle\}$ . Thus,  $\theta$  is the non-adiabatic geometric phase, which is half of the solid angle enclosed by the evolution path [64], as shown in Fig. 3(b).

### B. Steady entanglement with dissipative dynamics

In Rydberg atom system, the creation of steady-state entanglement via dissipation has been studied in Refs. [47, 65], where a weak microwave field is needed

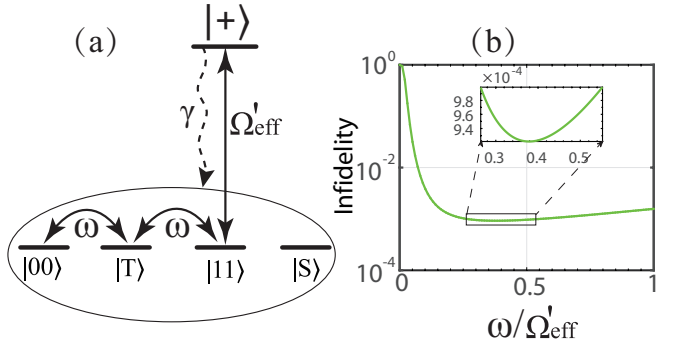


FIG. 4. (a) Dynamical processes to generate the steady entangled state through combining the unitary and dissipative dynamics. (b) Infidelity of the steady entangled state  $(|01\rangle - |10\rangle)/\sqrt{2}$  versus  $\omega/\Omega'_\text{eff}$ . The inter-atomic distance is set as  $3 \mu\text{m}$ . And the Rabi frequency is set as  $\Omega = 2\pi \times 1 \text{ MHz}$ . The value of  $\Delta$  is calculated through the modified RAB condition  $V_d = \sqrt{2}\Delta$ .

to drive resonantly the transition between two ground states  $|0\rangle$  and  $|1\rangle$ . Following the basic ideas of the schemes [47, 65], we here also consider that the two atoms are interacting with the microwave field as

$$\hat{H}_{\text{mw}} = \frac{\sqrt{2}\omega}{2} (|00\rangle + |11\rangle)\langle T| + \text{H.c.}, \quad (16)$$

where  $|T\rangle \equiv (|01\rangle + |10\rangle)/\sqrt{2}$  is a triplet Bell state. The singlet state  $|S\rangle \equiv (|01\rangle - |10\rangle)/\sqrt{2}$  is decoupled to Hamiltonian (16) and is the desired steady entangled state. We can learn from Eq. (16) that the microwave shuffles the states  $|00\rangle$ ,  $|T\rangle$ , and  $|11\rangle$ , but keeps  $|S\rangle$  invariant. Since the stark shifts do not influence the dissipative dynamics, we thus consider to turn the red-detuned laser off and modify the RAB condition as  $V_d = \sqrt{2}\Delta$ . The effective Hamiltonian that control unitary dynamics can be written as the form  $\hat{H}'_e = (\Omega'_\text{eff}/2)(|11\rangle\langle +| + \text{H.c.}) + \hat{S}$ , where  $\Omega'_\text{eff} = \sqrt{2}\Omega^2/(2\Delta)$  and  $\hat{S}$  denotes the stark shifts.

Combining the effective Hamiltonian  $\hat{H}'_e$  with the microwave Hamiltonian  $\hat{H}_{\text{mw}}$  in Eq. (16), and the dissipative dynamics as depicted in Fig. 4(a), the desired state  $|S\rangle$  would be prepared as the steady state of the system. In other words, once  $|S\rangle$  is occupied through the dissipative dynamics, the entangled state is created successfully. Otherwise, if the other three states are occupied, the unitary dynamics will excite the two atoms into  $|r_{pf}\rangle$  and then it decays to the ground subspace again. In Fig. 4(b), we plot the infidelity of the steady state via numerically solving the master equation (13) with initial Hamiltonian, and the practical parameters of RRI and atomic spontaneous emission rate. One can see that the fidelity is higher than 0.999 when the x-axis value range is in  $[0.26, 0.54]$ .

### C. Measurement of parameters

If  $C_3$  and the distance as well as laser parameters  $\Omega$  and  $\Delta$  are known, one can change the electric field strength to observe where the collective Rabi oscillation with the effective frequency  $\Omega^2/\Delta$  emerges. And inversely determine that whether the tuned electric field strength makes dipole-dipole interaction resonant or not.

Besides, if the electric field strength that make the resonant dipole-dipole interaction are known and set well in advance, one can scan the values of  $\Omega$  and  $\Delta$  to observe whether the RAB-based Rabi oscillation are achieved. And thus can inversely calculate the RRI strength and can further calculate the  $C_3$  parameter when the interatomic distance is known. Also, one can roughly estimate the inter-atomic distance if  $C_3$  is known.

### V. CONCLUSION

In conclusion, we have proposed how to construct the RAB dynamics with several types of resonant Rydberg dipole-dipole interaction by using the dressed state method. In contrast to the usual vdW-based RAB which is valid when the inter-atomic distance is larger than the characteristic distance  $R_c$  [4], our study is valid when the inter-atomic distance is less than the characteristic distance  $R_c$ , which makes the layout of RAB more complete. We also show the potential applications of the proposed RAB in geometric quantum computation, dissipative-dynamics based entanglement preparation, and the parameter estimation.

### ACKNOWLEDGEMENTS

The author would like to thank Dr. Jin-Lei Wu and Prof. Xiao-Qiang Shao for discussions, and Dr. Bao-Jie Liu for useful suggestions. This work was supported by National Natural Science Foundation of China (NSFC) under No.11804308 and China Postdoctoral Science Foundation (CPSF) under No. 2018T110735.

---

[1] T. F. Gallagher, *Rydberg atoms* (Cambridge University Press, 2005).

[2] D. Jaksch, J. I. Cirac, P. Zoller, S. L. Rolston, R. Côté, and M. D. Lukin, Phys. Rev. Lett. **85**, 2208 (2000).

[3] M. D. Lukin, M. Fleischhauer, R. Cote, L. M. Duan, D. Jaksch, J. I. Cirac, and P. Zoller, Phys. Rev. Lett. **87**, 037901 (2001).

[4] M. Saffman, T. G. Walker, and K. Mølmer, Rev. Mod. Phys. **82**, 2313 (2010).

[5] D. Comparat and P. Pillet, J. Opt. Soc. Am. B **27**, A208 (2010).

[6] M. Saffman, J. Phys. B: Atom. Mol. Opt. Phys. **49**, 202001 (2016).

[7] L. Isenhower, E. Urban, X. L. Zhang, A. T. Gill, T. Henage, T. A. Johnson, T. G. Walker, and M. Saffman, Phys. Rev. Lett. **104**, 010503 (2010).

[8] X. L. Zhang, L. Isenhower, A. T. Gill, T. G. Walker, and M. Saffman, Phys. Rev. A **82**, 030306 (2010).

[9] T. Wilk, A. Gaëtan, C. Evellin, J. Wolters, Y. Miroshnychenko, P. Grangier, and A. Browaeys, Phys. Rev. Lett. **104**, 010502 (2010).

[10] K. M. Maller, M. T. Lichtman, T. Xia, Y. Sun, M. J. Piotrowicz, A. W. Carr, L. Isenhower, and M. Saffman, Phys. Rev. A **92**, 022336 (2015).

[11] Y. Zeng, P. Xu, X. He, Y. Liu, M. Liu, J. Wang, D. J. Papoular, G. V. Shlyapnikov, and M. Zhan, Phys. Rev. Lett. **119**, 160502 (2017).

[12] C. J. Picken, R. Legaie, K. McDonnell, and J. D. Pritchard, Quan. Sci. Tech. **4**, 015011 (2018).

[13] H. Levine, A. Keesling, A. Omran, H. Bernien, S. Schwartz, A. S. Zibrov, M. Endres, M. Greiner, V. Vuletić, and M. D. Lukin, Phys. Rev. Lett. **121**, 123603 (2018).

[14] H. Levine, A. Keesling, G. Semeghini, A. Omran, T. T. Wang, S. Ebadi, H. Bernien, M. Greiner, V. Vuletić, H. Pichler, and M. D. Lukin, Phys. Rev. Lett. **123**, 170503 (2019).

[15] T. M. Graham, M. Kwon, B. Grinkemeyer, Z. Marra, X. Jiang, M. T. Lichtman, Y. Sun, M. Ebert, and M. Saffman, Phys. Rev. Lett. **123**, 230501 (2019).

[16] A. Omran, H. Levine, A. Keesling, G. Semeghini, T. T. Wang, S. Ebadi, H. Bernien, A. S. Zibrov, H. Pichler, S. Choi, J. Cui, M. Rossignolo, P. Rembold, S. Montangero, T. Calarco, M. Endres, M. Greiner, V. Vuletić, and M. D. Lukin, Science **365**, 570 (2019).

[17] C. Ates, T. Pohl, T. Pattard, and J. M. Rost, Phys. Rev. Lett. **98**, 023002 (2007).

[18] T. Amthor, C. Giese, C. S. Hofmann, and M. Weidmüller, Phys. Rev. Lett. **104**, 013001 (2010).

[19] T. Pohl and P. R. Berman, Phys. Rev. Lett. **102**, 013004 (2009).

[20] J. Qian, Y. Qian, M. Ke, X.-L. Feng, C. H. Oh, and Y. Wang, Phys. Rev. A **80**, 053413 (2009).

[21] X.-F. Shi, Phys. Rev. Applied **7**, 064017 (2017); Phys. Rev. Applied **11**, 044035 (2019).

[22] S. de Léséleuc, D. Barredo, V. Lienhard, A. Browaeys, and T. Lahaye, Phys. Rev. Lett. **119**, 053202 (2017).

[23] K. Afrousheh, P. Bohloli-Zanjani, D. Vagale, A. Mugford, M. Fedorov, and J. D. D. Martin, Phys. Rev. Lett. **93**, 233001 (2004).

[24] P. Bohloli-Zanjani, J. A. Petrus, and J. D. D. Martin, Phys. Rev. Lett. **98**, 203005 (2007).

[25] S. Sevinçli and T. Pohl, New J. Phys. **16**, 123036 (2014).

[26] M. Marcuzzi, E. Levi, W. Li, J. P. Garrahan, B. Olmos, and I. Lesanovsky, New J. Phys. **17**, 072003 (2015).

[27] F. M. Gambetta, W. Li, F. Schmidt-Kaler, and I. Lesanovsky, Phys. Rev. Lett. **124**, 043402 (2020).

[28] J. T. Young, P. Bienias, R. Belyansky, A. M. Kaufman, and A. V. Gorshkov, “Asymmetric blockade and multi-qubit gates via dipole-dipole interactions,” (2020), arXiv:2006.02486 [quant-ph].

[29] T. G. Walker and M. Saffman, J. Phys. B **38**, S309 (2005).

[30] T. Vogt, M. Viteau, A. Chotia, J. Zhao, D. Comparat, and P. Pillet, Phys. Rev. Lett. **99**, 073002 (2007).

[31] C. S. E. van Ditzhuijzen, A. F. Koenderink, J. V. Hernández, F. Robicheaux, L. D. Noordam, and H. B. v. L. van den Heuvell, Phys. Rev. Lett. **100**, 243201 (2008).

[32] I. I. Ryabtsev, D. B. Tretyakov, I. I. Beterov, and V. M. Entin, Phys. Rev. Lett. **104**, 073003 (2010).

[33] J. Nipper, J. B. Balewski, A. T. Krupp, B. Butscher, R. Löw, and T. Pfau, Phys. Rev. Lett. **108**, 113001 (2012).

[34] S. Ravets, H. Labuhn, D. Barredo, L. Béguin, T. Lahaye, and A. Browaeys, Nat. Phys. **10**, 914 (2014).

[35] S. Ravets, H. Labuhn, D. Barredo, T. Lahaye, and A. Browaeys, Phys. Rev. A **92**, 020701(R) (2015).

[36] Z. C. Liu, N. P. Inman, T. J. Carroll, and M. W. Noel, Phys. Rev. Lett. **124**, 133402 (2020).

[37] A. Browaeys, D. Barredo, and T. Lahaye, J. Phys. B: Atom., Mol. Opt. Phys. **49**, 152001 (2016).

[38] E. A. Yakshina, D. B. Tretyakov, I. I. Beterov, V. M. Entin, C. Andreeva, A. Cinins, A. Markovski, Z. Iftikhar, A. Ekers, and I. I. Ryabtsev, Phys. Rev. A **94**, 043417 (2016).

[39] H. Gorniacyk, C. Tresp, P. Bienias, A. Paris-Mandoki, W. Li, I. Mirgorodskiy, H. P. Büchler, I. Lesanovsky, and S. Hofferberth, Nat. Commu. **7**, 12480 (2016).

[40] I. I. Beterov, M. Saffman, E. A. Yakshina, D. B. Tretyakov, V. M. Entin, S. Bergamini, E. A. Kuznetsova, and I. I. Ryabtsev, Phys. Rev. A **94**, 062307 (2016).

[41] D. Petrosyan, F. Motzoi, M. Saffman, and K. Mølmer, Phys. Rev. A **96**, 042306 (2017).

[42] M. Khazali and K. Mølmer, Phys. Rev. X **10**, 021054 (2020).

[43] A. Paris-Mandoki, H. Gorniacyk, C. Tresp, I. Mirgorodskiy, and S. Hofferberth, J. Phys. B: Atom., Mol. Opt. Phys. **49**, 164001 (2016).

[44] Z. Zuo and K. Nakagawa, Phys. Rev. A **82**, 062328 (2010).

[45] T. E. Lee, H. Häffner, and M. C. Cross, Phys. Rev. Lett. **108**, 023602 (2012).

[46] W. Li, C. Ates, and I. Lesanovsky, Phys. Rev. Lett. **110**, 213005 (2013).

[47] A. W. Carr and M. Saffman, Phys. Rev. Lett. **111**, 033607 (2013).

[48] Y.-H. Chen, Z.-C. Shi, J. Song, Y. Xia, and S.-B. Zheng, Phys. Rev. A **97**, 032328 (2018); D. X. Li and X. Q. Shao, Phys. Rev. A **99**, 032348 (2019); C. Yang, D. Li, and X. Shao, Science China Physics, Mechanics & Astronomy **62**, 110312 (2019).

[49] R. Li, D. Yu, S.-L. Su, and J. Qian, Phys. Rev. A **101**, 042328 (2020).

[50] S. Basak, Y. Chougale, and R. Nath, Phys. Rev. Lett. **120**, 123204 (2018).

[51] S.-L. Su, Y. Gao, E. Liang, and S. Zhang, Phys. Rev. A **95**, 022319 (2017); S. L. Su, H. Z. Shen, E. Liang, and S. Zhang, Phys. Rev. A **98**, 032306 (2018); S.-L. Su, F.-Q. Guo, L. Tian, X.-Y. Zhu, L.-L. Yan, E.-J. Liang, and M. Feng, Phys. Rev. A **101**, 012347 (2020); J.-L. Wu, S.-L. Su, Y. Wang, J. Song, Y. Xia, and Y.-Y. Jiang, Opt. Lett. **45**, 1200 (2020).

[52] S. Bai, X. Tian, X. Han, Y. Jiao, J. Wu, J. Zhao, and S. Jia, New J. Phys. **22**, 013004 (2020).

[53] F. M. Gambetta, C. Zhang, M. Hennrich, I. Lesanovsky, and W. Li, (2020), arXiv:2005.05726 [cond-mat.quant-gas].

[54] J. Taylor, J. Sinclair, K. Bonsma-Fisher, D. England, M. Spanner, and K. Heshami, (2019), arXiv:1912.05675 [physics.atom-ph].

[55] D. Barredo, H. Labuhn, S. Ravets, T. Lahaye, A. Browaeys, and C. S. Adams, Phys. Rev. Lett. **114**, 113002 (2015).

[56] J.-L. Wu, J. Song, and S.-L. Su, Phys. Lett. A **383**, 126039 (2019).

[57] C. E. Theodosiou, Phys. Rev. A **30**, 2881 (1984).

[58] I. I. Beterov, I. I. Ryabtsev, D. B. Tretyakov, and V. M. Entin, Phys. Rev. A **79**, 052504 (2009).

[59] E. Sjöqvist, D. M. Tong, L. M. Andersson, B. Hessmo, M. Johansson, and K. Singh, New J. Phys. **14**, 103035 (2012).

[60] G. F. Xu, J. Zhang, D. M. Tong, E. Sjöqvist, and L. C. Kwek, Phys. Rev. Lett. **109**, 170501 (2012).

[61] Z.-Y. Xue, J. Zhou, Y.-M. Chu, and Y. Hu, Phys. Rev. A **94**, 022331 (2016).

[62] P. Z. Zhao, X.-D. Cui, G. F. Xu, E. Sjöqvist, and D. M. Tong, Phys. Rev. A **96**, 052316 (2017).

[63] B.-J. Liu, X.-K. Song, Z.-Y. Xue, X. Wang, and M.-H. Yung, Phys. Rev. Lett. **123**, 100501 (2019).

[64] Y. Aharonov and J. Anandan, Phys. Rev. Lett. **58**, 1593 (1987).

[65] D. D. B. Rao and K. Mølmer, Phys. Rev. Lett. **111**, 033606 (2013).